Available online at www.sciencedirect.com
ScienceDirect
Biochimica et Biophysica Acta 1778 (2008) 549–558
Biochimica et Biophysica Acta
BBA
www.elsevier.com/locate/bbamem

# Responding double-porous lipid membrane: Lyotropic phases in a polymer scaffold

Christoffer Åberg [a,*], Cécile Pairin [a], Fátima O. Costa-Balogh [a,b], Emma Sparr [a]

[a] Division of Physical Chemistry 1, Chemical Center, Lund University, P.O. Box 124, SE-22100 Lund, Sweden
[b] Centro de Estudos Farmacêuticos, Faculdade de Farmácia, Universidade de Coimbra, Coimbra codex P-3004-535, Portugal

Received 6 July 2007; received in revised form 28 September 2007; accepted 12 October 2007
Available online 1 November 2007

**Abstract**

The large osmotic gradient over the outermost layer of human skin implies major structural changes along the gradient, which in turn affects transport. In particular, the possibility of phase changes introduces a non-linear element to the transport behaviour. We present a novel model membrane system to be used for studying these transport mechanisms, where we use a hydrophobic porous polymer membrane as a scaffold for lipid lyotropic phases. The polymer membrane provides mechanical robustness, but also prevents defects of the lipid lyotropic phases, and it can induce an orientation of anisotropic phases. We study the location, structure and phase behaviour of the confined phases. It is shown that this model membrane system allow for accurate measurements of transport through lipid membranes in the presence of different osmotic gradients. A theoretical description is evaluated and shows that this phenomenon can be understood in terms of the proposed mechanism of phase changes. The novel double-porous lipid membrane constitutes a mechanically robust system for studies in aligned systems, which is generally very difficult to achieve. This could have large implications for studies of transport processes in, e.g. skin and other biomembrane model systems.


*Keywords:* Diffusive transport; Permeability; Osmotic gradient; Phase transformation; Stratum corneum; Responding membrane

## 1. Introduction

In land-living mammals the skin serves as a protective transport barrier. A main function is to allow for a careful regulation of a constant chemical potential of water inside the body irrespective of the external conditions. The skin also serves as a protection from many other molecular species, natural or anthropogenic. It is worth noting that for respiratory gases, $CO_2$ and $O_2$, a transport across the skin is typically functionally beneficial since it reduces the load on lung respiration. Furthermore there can also be great advantages in the administration of drugs through the skin. Such a balance between needs for protection and possibilities of molecular transport provides a driving force for developing a regulatory mechanism.

Inside our body there is a water-rich environment, with an essentially uniform water chemical potential corresponding to that of physiological saline (0.15 M NaCl) or equivalently 99.5% relative humidity (RH). In general the ambient atmosphere is much drier with typical values in the range 40% to 90% RH. It is an amazing fact that the gradient in water chemical potential is concentrated to the only 10–20 $\mu$m thick outermost layer of the skin — the stratum corneum [1]. It consists of dead cells (corneocytes) embedded in a lipid multilamellar matrix, where the bilayers are arranged parallel to the skin surface [2]. The extracellular lipids constitute the only continuous region of the stratum corneum. A molecular transport across the skin thus necessarily involves a step of passing the lipid structure [3–5]. An effect of the lamellar organisation is a major reduction in permeability for strongly polar or apolar substances, whereas those of intermediate polarity pass more readily.

The gradients across the stratum corneum can have major implications on its function. The gradient in water chemical potential causes a heterogeneous swelling of the lipid matrix. This, in turn, can affect the transport of other molecules, like metabolites or transdermal drugs. Furthermore, there is also the possibility of phase transformations, e.g. between a liquid

* Corresponding author. Tel.: +46 46 222 15 36.
*E-mail address:* christoffer.aberg@gmail.com (C. Åberg).

0005-2736/$ - see front matter © 2007 Elsevier B.V. All rights reserved.
doi:10.1016/j.bbamem.2007.10.020

crystalline phase and a gel phase, induced by the variation in water chemical potential along the barrier [6,7]. Phase transformations introduce a non-linear element to the water transport and this behaviour has been seen experimentally for stratum corneum [8,9]. It will also affect the transport of other molecules, giving rise to higher permeability at higher hydration, as observed experimentally for stratum corneum and model membranes of stratum corneum lipids [8,10]. In this way, the barrier membrane of stratum corneum responds to the gradient in water chemical potential.

The stratum corneum can be seen as an example of a more general class of complex barriers with non-linear transport properties — responding membranes [11,12]. These membranes are modulated by variations in the compositions of the surrounding media, which cause structural changes in the barrier membrane. In a previous study we have demonstrated the qualitative effect on diffusional transport induced by the occurrence of a phase change in the barrier membrane [13]. This was achieved by casting a liquid crystalline monoolein sample on a mechanical support separating two compartments containing aqueous solutions of poly(ethylene glycol) of controlled osmotic pressures (physically equivalent to controlled water chemical potentials). At high osmotic pressures the monoolein–water system changes from a bicontinuous cubic to a lamellar structure. In the cubic phase diffusional transport is uninhibited due to the existence of three-dimensional pathways for both polar and apolar substances. In a lamellar system, on the other hand, strongly polar and strongly apolar substances experience a substantial hindrance for diffusion normal to the orientation of the lamellar plane.

Although the experiments with the cast liquid crystalline film gave satisfactory qualitative results demonstrating the significance of a phase change, there were clear difficulties with the method related to the quantitative reliability: The diameter of the cast sample was >1 mm which made it difficult to ensure that the emerging lamellar phase oriented uniformly parallel to the support. Furthermore local defects can easily occur and these can have strong effects on the transport. The system is also mechanically fragile reducing the possibilities for stirring.

In this work we present a novel model membrane system that presents a solution to these problems. The basic idea is the use of a porous, micron size, polymer membrane as a scaffold for the lipid liquid crystalline structure, thereby creating what we call a *double-porous membrane*. (See Fig. 1 below for a schematic comparison of the two methods.) Primarily this provides mechanical stability, but by appropriately choosing the polymer material one can also obtain a surface-induced orientation of anisotropic liquid crystalline phases. There is a tight molecular coupling between the scaffold of the polymer porous material and the lipid phases eliminating edge defects and also reducing the occurrence of defects in the bulk. In this way we can monitor not only the effects of phase changes but also of structural variations within a phase. The double-porous membrane system is hence very suitable for quantitative and accurate measurements of transport across oriented liquid crystalline phases. It can be valuable in the applications of high through-put measurements of drug transport across model membranes [14]. To support this conclusion, we use the same lipid system as previously studied. The location and phase behaviour of the lipids in the membrane as well as the transport in the presence of an osmotic gradient is investigated. A theoretical analysis of non-linear transport due to structural changes induced by an external osmotic gradient is given. As a special case, transport through the double-porous membrane is described. The fact that the lyotropic phases are confined within the polymer scaffold does complicate the analysis slightly, but we show that such effects can be accounted for.

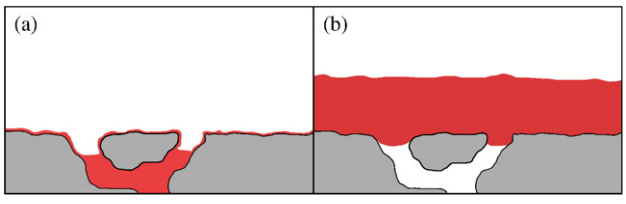


Fig. 1. Schematic comparison of model lipid membranes prepared by different methods. (a) Double-porous membrane where the lipids are confined within the synthetic support membrane. (b) A lipid membrane formed on top of the support membrane. This is expected when the lipids are added from a solvent that does not fully wet the support membrane (as in Ref. [13]). Note: not to scale.

Table 1
PEG 8000 concentration in mass per total solution volume, the corresponding osmotic pressure calculated from aqueous PEG 8000 density measurements [19] and osmotic pressure data [15], and corresponding monoolein–water equilibrium phase behaviour

| PEG 8000 conc/gl$^{-1}$ | Π/MPa | Phase behaviour |
|---|---|---|
| 200 | 0.66 | Cubic |
| 250 | 1.11 | Cubic |
| 300 | 1.75 | Cubic |
| 350 | 2.64 | Cubic |
| 370 | 3.09 | Lamellar |
| 400 | 3.87 | Lamellar |
| 420 | 4.47 | Lamellar |

## 2. Materials and methods

### 2.1. Materials

Poly(ethylene glycol) 8000 (PEG 8000) was purchased from Aldrich (Sweden, lot 10228AC-285). PEG is a commonly used polymer in osmotic stress experiments, and the osmotic pressure is available in the literature (Table 1) [15].

Monoolein was a kind gift from Axel Borerup, Danisco Ingredients (Denmark). The monoolein (batch 173403) is of technical grade and it consists of ca 95% monoglycerides and the rest is mainly diglycerides, fatty acids and free glycerol. The monoolein content is ca 90%. The phase behaviour of this and similar commercial samples from the same source is well characterised, and it is similar to that of pure monoolein, although the exact positions of the phase boundary are slightly shifted [16–18]. The bulk phase behaviour of the batch was checked by letting samples of hydrated monoolein (around 30 wt.%) equilibrate inside a dialysis membrane (Spectra/Por, lot 09593, cut-off 1000) with aqueous solutions of PEG 8000 of different concentrations. Visual inspection, also using polarised light, shows that only an isotropic phase is present at osmotic pressures below 2.64 MPa, whereas at osmotic pressures above 3.09 MPa an anisotropic phase is detected (Table 1). This gives an estimate of the position of the inverted cubic Ia3d to the liquid crystalline $L_\alpha$ lamellar phase transition. This is slightly different from previous results; with a monoolein content of 95% Ref. [13] reported the range 2.16–2.64 MPa (recalculated with

the help of Refs. [19] and [15] as in Table 1), and with a monoolein content of 99% the phase transition occurs at 2.78 MPa [20].

Eosin was purchased from Kebo (Sweden, A1344) and rhodamine-PE was obtained from Molecular probes (Netherlands).

The water used was from a Milli-Q filtration system (Millipore).

### 2.2. Preparation of double-porous membranes

Polyvinylidene fluoride (PVF) membranes were purchased from Millipore (pore diameter 0.45 $\mu$m, porousity 75%, diameter 25 mm), and dipped once in a solution of monoolein dissolved in methanol/chloroform (1:1 by volume) with a concentration of 0.5 g/ml. Evaporation of the solvent was performed in vacuum (>4 h). The membranes were weighed before and after preparation to determine the amount of monoolein inside the pores (25–28 mg).

For membranes prepared with half the amount of monoolein, a lower concentration of lipid in the methanol/chloroform solution (0.25 g/ml) was used.

For the development of the double-porous membrane, a number of different synthetic polymer membranes (polyvinylidene fluoride, vinyl/acrylic polymer, polypropylene, polyethersulfone, mixed cellulose ester, polytetrafluoroethylene, zeflour, nylon, teflon) with different porous structures and pore sizes (0.4–40 $\mu$m) were explored. Different ways of spreading lipids inside the pores were investigated, including dipping or spin coating of an isotropic lipid melt (>40 °C) or lipids dissolved in chloroform/methanol.

The preparation procedure for the double-porous membrane described above was found superior with respect to lipid confinement inside the pores, apparent surface induced orientation, robustness and resistance to solvents.

### 2.3. Confocal laser scanning microscopy

Experiments were carried out on a Nikon Diaphot 300/BioRad MRC 1024 confocal laser scanning microscope. Images of each plane were collected in steps of 2 $\mu$m up to a total of 5 $\mu$m.

Samples were prepared by dipping a PVF membrane once in a solution of monoolein and the fluorescent lipid analogue rhodamine-PE dissolved in methanol/chloroform (1:1 by volume). The total concentration of lipids was the same as above, 0.5 g/ml, with a ratio of lipid analogue to total number of lipids of $10^{-3}$. Evaporation of the solvent was performed in vacuum (>4 h), and the membrane was thereafter carefully hydrated in Milli-Q water.

### 2.4. SAXS

Small angle X-ray scattering (SAXS) experiments were carried out at MAXLab (Lund, Sweden), beamline I711, with a single crystal monochromator. A wavelength of 1.08 Å and a beam spot-size of approximately 79 $\mu$m were used. For data collection a Marresearch CCD detector was used with a sample-to-detector distance of 1456 mm. In our setup the scattering vector $q$ was limited by 3 $nm^{-1}$ from above.

Samples were prepared by exposing hydrated double-porous membranes, prepared as described above, to aqueous solutions of PEG 8000 of different concentrations for 12 h. A piece of the membrane was then cut and placed between mica plates in a solid sample holder.

### 2.5. Transport experiments

We used a setup of Franz diffusion cells (8 ml receptor volume, 0.636 $cm^2$ diffusion area) from Permegear, Inc. (Bethlehem, PA, USA). Both the receptor and the donor chambers were filled with aqueous solutions of PEG 8000 with different concentrations. During the experiment the donor chamber also contained eosin (1 mg/ml) and was covered with parafilm. The two chambers were separated by a double-porous lipid membrane, prepared as described above, and carefully hydrated with two or three drops of water. The system was left to reach steady state in the osmotic gradient for 12 h, after which the donor solutions were replaced by aqueous solutions containing eosin and the same concentration of PEG 8000. In the experimental setup, care was taken to ensure that no air bubbles were trapped under the membrane. Experiments were performed at room temperature, and lasted for about 24 h.

In order to maintain steady-state conditions, constant boundary conditions in both eosin concentration and osmotic pressure at both sides of the double-porous membrane must be ensured. Hence, the solution in the donor chamber was regularly exchanged with fresh solutions with the same PEG 8000 and eosin concentration. The solution in the receptor chamber was magnetically stirred, and large enough (about 22 ml including the tubes to and from the spectrophotometer) to maintain sink conditions. The osmotic stress causes dehydration of the lipid membrane, and under these conditions the system is heterogeneous. Hence, this system is defined by the osmotic gradient and not by the composition (water content) of the membrane. The amount of water released/taken up due to the dehydration/hydration of the membrane is negligible compared to the sizes of the receptor and donor cells, so it can be safely assumed that it does not affect the overall osmotic gradient.

The amount of eosin that diffused through the membrane was continuously measured by UV/visible spectrophotometry (Perkin-Elmer UV/VIS Spectrometer Lambda 14; Peristaltic pump Ismatec, 4 channels) at 521 nm. From this the flux at steady state was deduced from the slope of the linear part of the concentration in the receptor chamber as a function of time. Data is presented in terms of the permeability of the membrane to eosin, $P_i$, defined by

$$J_i = -P_i \Delta c_i \quad (1)$$

where $J_i$ (mol/$m^2$s) and $c_i$ (mol/$m^3$) is the flux and concentration gradient, respectively, of eosin.

## 3. Results and discussion

### 3.1. Double-porous membrane

The aim is to prepare a membrane where lyotropic lipid phases are confined inside the porous structure of a synthetic support membrane, thus forming a double-porous structure (see Fig. 1a for a schematic illustration). This preparation requires both a homogeneous distribution of the lipid material inside the porous support membrane, and the formation of highly structured lyotropic phases upon hydration. We chose to use a hydrophobic support membrane, and to add the lipids from a non-polar solvent (chloroform/methanol) that readily wets this membrane.

We chose monoolein as a model lipid, since there is a large body of experimental data for the monoolein–water system [21,22,17,23,20]. Furthermore, the water transport through the Ia3d cubic phase has been studied previously [24]. This greatly facilitates the theoretical modelling of the experiments.

To verify that the lipids distribute homogeneously inside the membrane, samples prepared with a trace amount of fluorescent lipid analogue, rhodamine-PE, were investigated by means of confocal laser scanning microscopy. As shown in Fig. 2, fluorescence was clearly detected within a 120 $\mu$m thick part of the

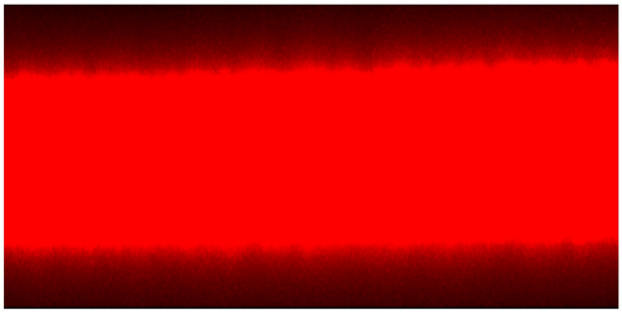

Fig. 2. $z$-stack of confocal scanning microscopy images of a double-porous membrane. The higher intensity in the central part of the membrane corresponds to a higher concentration of the fluorescent lipid analogue. Full height of image corresponds to around 120 $\mu$m.

membrane. This is close to the membrane thickness 125 μm. With the same solvent and a hydrophilic membrane, as the one used in Ref. [13], the lipids would instead arrange themselves on the exterior membrane surface, as schematically illustrated in Fig. 1b. This was also confirmed by confocal scanning microscopy (data not shown).

These experiments also showed that the lipids are rather homogeneously distributed in the central part of the double-porous membrane. However, closer to the exterior surface a decrease in fluorescence intensity was found. We believe that the explanation for this lies in the surface activity of the lipids. The lipids preferentially form a monolayer on *all* hydrophobic surfaces of the membrane, both the exterior surface and the pore wall surfaces. The remaining lipids fill the central part of the pores. Again, see Fig. 1a for an illustration. Water wets the double-porous membrane, in contrast to the bare hydrophobic support membrane. This observation supports that the exterior surface is covered by a lipid monolayer.

A transport study using membranes with varying amounts of monoolein inside the pores further supports this view. If we ignore the possibility that some lipids form a monolayer covering all hydrophobic surfaces, then halving the amount of monoolein would mean that also the effective thickness is halved, and hence the permeability doubled. However, if one takes into account that there is a substantial amount of lipids forming a monolayer covering both the membrane exterior surface and pore wall surfaces, this simple inverse proportionality will not hold anymore. Indeed, it was observed that halving the amount of monoolein caused a tripled permeability of eosin, consistent with this reasoning. These experiments were performed for homogeneously swollen cubic phases (osmotic pressure 0.66 MPa in both receptor and donor chambers).

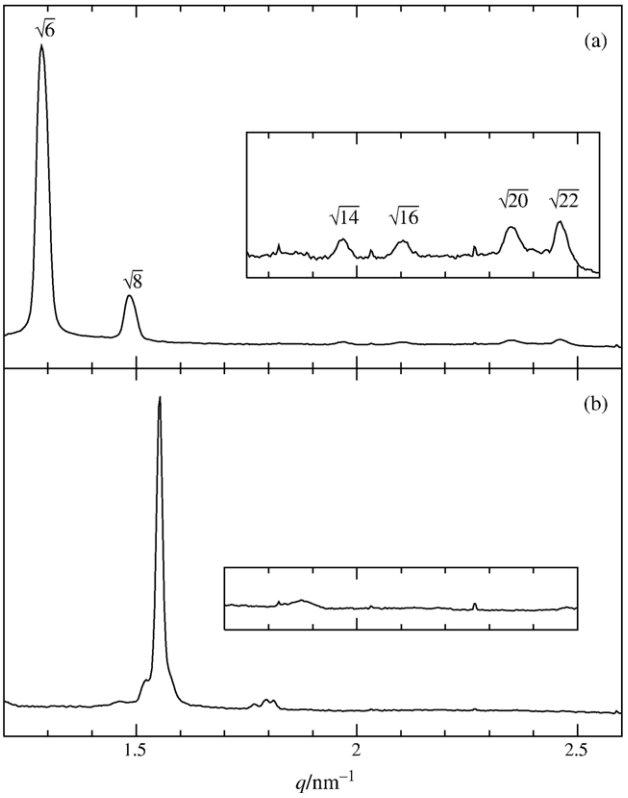


Fig. 3. Results of SAXS study for double-porous membranes equilibrated at different osmotic pressures. (a) 0.66 MPa. The diffraction pattern is consistent with an Ia3d cubic phase, as expected from bulk behaviour, with a unit cell size of 120 Å. Inset shows a vertical enlargement of the part of the spectrum below it (using the same horizontal scale). (b) 4.47 MPa. The major peak is interpreted as the first order peak from an $L_\alpha$ lamellar phase with a repeat-distance of 40.5 Å. Higher order peaks cannot be seen because of the limited $q$-range. Inset shows (using the same horizontal scale) the diffraction pattern obtained for a dry support membrane for comparison. Note that vertical scales are not comparable.

### 3.2. Structure and phase behaviour inside pores

In the porous membrane there is a large contact area between the lipid phase and the support. Potentially the surface interaction can be strong enough to affect the bulk phase equilibria of the lipids [25]. In order to investigate this possibility, SAXS studies were performed with double-porous membranes equilibrated at different osmotic pressures. Fig. 3a shows the diffraction pattern obtained at osmotic pressure 0.66 MPa. This pattern with six diffraction peaks is consistent with an Ia3d cubic structure with a lattice parameter of 120 Å.

Fig. 3b shows the registered diffraction at osmotic pressure 4.47 MPa. The diffraction pattern is clearly different, with one major peak. We interpret this as coming from an $L_\alpha$ lamellar phase with a repeat distance of about 40.5 Å. Higher order peaks cannot be seen because of the limited $q$-range.

A small peak at around 1.52 $nm^{-1}$ is also observed. The origin of this is not known. One possible explanation for this peak could be the presence of a co-existing lamellar phase that is slightly more swollen than the dominant lamellar phase at 1.55 $nm^{-1}$ (compare e.g. Ref. [26]), and it could be induced by e.g. the presence of trace fatty acids in the technical grade monoolein, or by the surface of the pore walls. The minor peak at 1.80 $nm^{-1}$ is also observed, though slightly shifted, in a control experiment with a dry bare support membrane (see inset in Fig. 3b). We thus believe that this peak originates from a structure in the support membrane itself. When filled with the liquid crystalline phase the structure of the support membrane might be slightly altered, explaining the small shift compared to the control experiment. This was not investigated further.

From these experiments, we can conclude that the same phases as found in bulk are formed also inside the pores. We further conclude that the measured lattice parameter for the Ia3d cubic phase is similar to previously reported data (around 125 Å) for bulk monoolein at the same osmotic pressure [23]. The lamellar repeat distance in bulk at water contents ranging from 5 to 20% (25 °C) has been reported as 35–45 Å [22], which is also in agreement with the present data. For more quantitative comparisons, we note that most studies report repeat distance as a function of water content, and that the relation between water content and osmotic stress is non-trivial.

For the lamellar phase, we are not aware of any such data, but the repulsive force dominating the interaction between bilayers at short-range has been measured as function of the ratio of water to monoolein molecules $n_w/n_l$ [20]. This interaction force,

which is physically equivalent to the osmotic pressure of the lamellar phase, is found to vary exponentially

$$\Pi = \frac{\text{force}}{\text{area}} = F_0 e^{-(n_w/n_l)/\lambda}$$

with $F_0$=42.7 MPa and $\lambda$=1.2 at 25 °C [20]. This can be recast into an osmotic pressure versus distance relation by the assumption of incompressibility of the lipid and water components. Under this assumption one readily finds from pure geometry that the ratio of water to lipid molecules is given by

$$\frac{n_w}{n_l} = \frac{(A_{lhg} N_A) h}{2\overline{V}_w}$$

where $A_{lhg}$=34.7 Å$^2$ is the area per lipid headgroup [27], $h$ the distance between lamellae and $\overline{V}_w = 1.802 \cdot 10^{-5}$ m$^3$/mol the molar volume of water. Then

$$\Pi = F_0 \exp\left(-\frac{(A_{lhg} N_A) h}{2\overline{V}_w} / \lambda\right).$$

From this, $h$ is easily found to be about 5 Å. With a bilayer thickness of approximately 34 Å [18,28] this shows agreement with the measured repeat-spacing. We thus conclude that the interaction between the lipids and the polymer support membrane has a negligible effect on the lipid phase equilibrium.

### 3.3. Orientation of the confined lamellar phase

Although the support membrane shows no effect on the lipid phase equilibrium, there is still the interesting fact that the surface free energy of the lamellar phase depends upon the orientation to consider. This means that the interaction with the wall in general should promote one particular orientation of the lamellae. Orientation in this context refers to the *local* orientation, i.e. how the phase is oriented with respect to the pore walls at a particular point. We envision that either the bilayers are oriented with the bilayer normal parallel to the pore walls, or form concentric cylinders in the pores. A priori we cannot predict which one is preferred, but by the preparation procedure described we hope to avoid a completely random orientation.

In order to test this, transport through a homogeneously swollen cubic double-porous membrane was compared with that through a homogeneously swollen lamellar double-porous membrane. For the interpretation of this, we note that the anisotropy of the lamellar phase implies that transport through it is highly affected by its local orientation. In the direction perpendicular to the bilayer plane, transport is significantly lower for any substance that does not partition equally between a lipid and an aqueous phase. In fact, one can show that at steady state the permeability, $P_i$, of a lamellar phase consisting of bilayers of a total thickness $L$ and water layers of a total thickness $W$ is given by [11]

$$\frac{1}{P_i} = \frac{L}{K_i D_i^l} + \frac{W}{D_i^w}$$

where $K_i$ is the partition coefficient between a lipid phase and an aqueous phase, and $D_i^l$ and $D_i^w$ is the diffusion coefficient in the lipid and aqueous region, respectively. Diffusion in the $L_\alpha$ bilayer means diffusion through a liquid crystalline phase, which typically is as rapid as in water. If we hence assume approximately equal diffusion coefficients, we see that the above expression predicts a strong dependence on the partition coefficient, $K_i$.

On the other hand, we do not expect such a strong dependence on $K_i$ when considering transport through a lamellar phase in a direction perpendicular to the bilayer normal. Irrespective of how the substance partitions, there exists a preferred channel — either the water layers, or the bilayers. The same holds true for the Ia3d cubic phase, since the bicontinuity ensures a continuous path through either the water or the lipid structure, though its isotropy makes transport independent of orientation. In both cases, diffusive transport is typically rapid. By comparing the permeability of the lamellar and cubic phases to a substance that does not partition equally, we should thus be able to deduce qualitative information regarding the local orientation of the lamellar phase.

Eosin has a partition coefficient between octanol and water of $6.3 \cdot 10^{-3}$ [13]. If we assume that it partitions similarly between the monoolein bilayer and water, its permeability should be rather sensitive to the orientation of the lamellar phase. At a low osmotic pressure (1.11 MPa), where the cubic phase forms, we find a permeability of 2.92 nm/s.

From this we conclude that transport through the double-porous membrane is feasible, and not hindered by the porous scaffold itself. Furthermore, it shows that transport of eosin through the rather narrow channels of the cubic phase is possible. This fact is important also for transport through the lamellar phase: If eosin would be too large to go through the narrow water channels of the lamellar phase, both orientations are likely to have a high permeability, and it might be hard to distinguish between them. However, the water channels of the cubic phase are comparable in size to those of the lamellar phase[1]. Hence the fact that eosin is able to pass through the cubic phase implies that it will also be able to pass through the lamellar phase, and the possibility that both orientations of the lamellar phase might give a low permeability due to narrow channels can be excluded.

At osmotic pressure 3.87 MPa, well beyond the cubic to lamellar phase transition in bulk, no flux of eosin was detected for 24 h, indicating that the major part of the lamellar phase is oriented with the bilayer normal parallel to the pore walls. Furthermore, defects in the bilayer system appear uncommon. These would, if ubiquitous, provide an extra channel through the lamellar phase and thus significantly increase its permeability.

[1] This can be shown from experimental data following the procedure outlined in Ref. [18] for the Pn3m cubic phase. Adjusting for the case of the Ia3d cubic phase we find that the water channel radius $r_w = 0.248a - l_m$, where $a$ is the size of the unit cell, and the factor 0.248 comes from the differential geometry of the minimal surface [29]. With experimental values it follows that the water channel sizes are approximately equal at the position of the phase transition. The variation with osmotic pressure can be found from the modeling below.

We note that the orientation of the pores with respect to the membrane surface plays a minor role when comparing transport through the two phases. It is true that a tortuous path increases the diffusion distance, and thus has a quantitative effect on transport (as discussed in more detail in Section 3.5). However, on a molecular scale diffusion through the lamellar phase is still in the direction parallel to the bilayer normal, and how the pore walls are oriented shows only a small effect. A similar conclusion holds for the cubic phase. Thus, relatively speaking, the pore orientation has little effect.

### 3.4. Transport in the presence of an external osmotic gradient

When the double-porous membrane is exposed to an osmotic gradient, there is not only a heterogeneous structure of the lyotropic phases as we pass along the membrane — there is also the possibility of heterogeneous *phase behaviour*, as schematically shown in Fig. 4. This, in turn, affects transport of water and other substances. A dramatic decrease in permeability can be found at the phase transition [13].

To demonstrate this experimentally, individual transport experiments were performed with the osmotic pressure of the donor chamber, $\Pi_D$, varying between 1.75 MPa and 4.47 MPa. The osmotic pressure in the receptor chamber was kept at 1.11 MPa in all experiments. This means that the starting experiment is a heterogeneously swollen cubic phase, since the osmotic pressure on each side of the membrane corresponds to a different unit cell size. For experiments where $\Pi_D$ is above the cubic to lamellar phase transition, we find not only a heterogeneous structure, but also heterogeneous phase behaviour, as the layer closest to the donor chamber forms a lamellar phase.

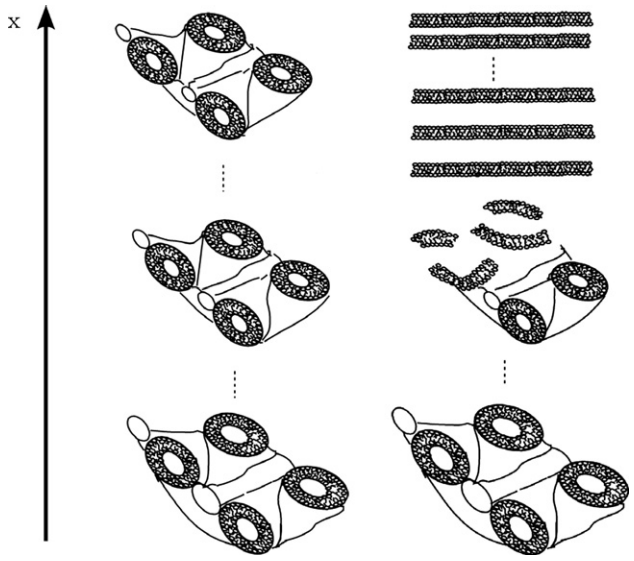


Fig. 4. Schematic illustration of the membrane structure as a function of position along the gradient. The osmotic pressure on the lower side is kept constant, while the osmotic pressure on the upper side is varied. (left) When the varied osmotic pressure is below the cubic to lamellar phase transition, all of the membrane is in the cubic phase. Due to the gradient, the size of a unit cell decreases with $x$. (right) When the upper osmotic pressure is above the phase transition, the upper part of the membrane is in the lamellar phase. Also the lamellar phase shows a decreasing swelling with $x$.

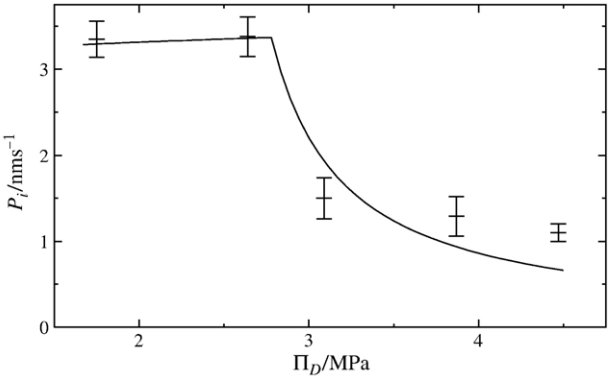


Fig. 5. Permeability, $P_i$, of the double-porous membrane to eosin as a function of varying osmotic gradient. $\Pi_D$ denotes the osmotic pressure of the donor chamber; the osmotic pressure of the receptor chamber was kept constant at 1.11 MPa. Data points are experimental results expressed as mean±standard deviation, each experiment carried out at least in duplicate. Solid curve shows the result of the theoretical model.

This heterogeneous swelling and phase behaviour has dramatic effects on transport of other substances. Fig. 5 shows experimental data for the permeability of eosin in the double-porous membrane with varying osmotic gradients. A clear steplike decrease in permeability is seen between $\Pi_D$=2.64 and 3.09 MPa. This range in osmotic pressure coincides with that found for the Ia3d to $L_\alpha$ phase transition in bulk. The diffusion characteristics of the cubic and lamellar phases are distinctly different for a substance that does not partition equally between lipid and aqueous layers. The introduction of only a few bilayers of the lamellar phase on the donor side gives rise to this marked decrease in permeability.

The same transport behaviour was earlier demonstrated for a monoolein membrane where the lyotropic phases were spread on a support membrane, and not present inside the pores [13]. However, in the current experiments we observe that the permeability decreases with the number of bilayers as the osmotic gradient is increased. This is also expected on a theoretical basis, as described below. The decrease in permeability with increasing osmotic gradient was not detected in the previous studies [13]. We believe the reason for this is a more well-defined orientation of the lamellar phase with less defects, when confined inside the pores of the scaffold membrane in the double-porous membrane.

### 3.5. Responding lipid membranes — theoretical considerations

We have previously [11–13] presented theoretical models for the steady-state diffusion of a substance through lipid membranes exposed to an external osmotic gradient. Central to these works are the assumptions of local thermodynamical equilibrium and steady-state flux of water. In the following, a unified presentation is given where these assumptions are explicitly developed into a general model, that essentially contains earlier models as special cases. At the end we explicitly focus on the case of a monoolein membrane, and discuss the influence of the porous membrane. For this last part, in particular, we wish to

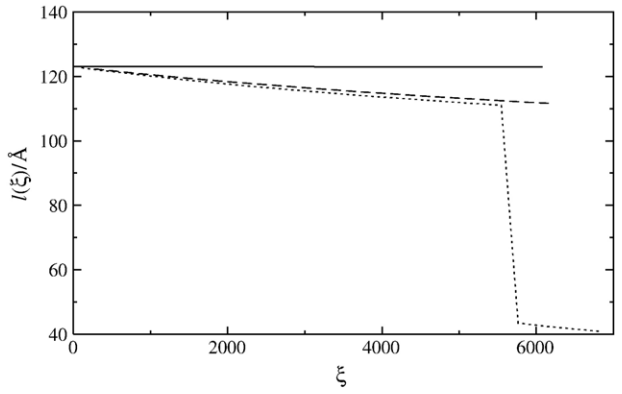


Fig. 6. The effect of the osmotic gradient on membrane structure. ξ measures the number of unit cells and repeat-spacings of the cubic and lamellar phase, respectively. Thus the local length $l(\xi)$ corresponds to the unit cell size or repeat-spacing. The solid line shows a homogeneously swollen cubic phase. Increasing the osmotic gradient leads to a heterogeneous swelling (dashed line). Increasing the osmotic gradient beyond the cubic to lamellar phase transition leads to the introduction of a lamellar phase (dotted curve). For illustrative purposes, the number of bilayers has here been exaggerated by increasing the permeability of a bilayer to water two orders of magnitude; the actual total number of bilayers is roughly ten at the highest osmotic gradient studied.

show that even though the porous membrane complicates the analysis, it is still possible to make a theoretical comparison.

The assumption of local thermodynamical equilibrium implies a heterogeneous structure and, possibly, heterogeneous phase behaviour along the gradient. In a quantitative discussion, this heterogeneity makes it convenient to introduce a dimensionless variable ξ to describe the position along the membrane; the actual position is then found from integrating a length function $l(\xi)$ that describes the local swelling. (This is illustrated for our particular case in Fig. 6 below.)

For the second substance *i*, we further assume that it does not affect the local thermodynamics, and write the total permeability, $P_i$, as an integral

$$\frac{1}{P_i}\int \frac{1}{P_i(\xi)}d\xi \tag{2}$$

of the local permeabilities $P_i(\xi)$ over the introduced ξ. Since transport is along the variable ξ one has to add the inverse local permeabilities to obtain the inverse total permeability [30].

By the assumption that the second substance does not affect the local thermodynamics, it follows, for a constant total amount of lipids $n_{l\mathrm{Tot}}$, that the structure and phase behaviour are solely determined by the local chemical potential of water $\mu_w$. This is also what we control experimentally in terms of the osmotic pressure Π, related to the water chemical potential by $-\bar{V}_w\Pi=\mu_w-\mu_w^0$, where $\mu_w^0$ is the chemical potential of pure water and $\bar{V}_w$ the molar volume of water. In terms of $\mu_w$ Eq. (2) becomes

$$\frac{1}{P_i}=\int_{\xi(\mu_R)}^{\xi(\mu_D)}\frac{1}{P_i(\mu_w)}\frac{d\xi}{d\mu_w}d\mu_w. \tag{3}$$

where $\mu_R$ and $\mu_D$ are the water chemical potentials in the receptor and donor chamber, respectively. The derivative $\frac{d\xi}{d\mu_w}$ is what connects a structural unit with its thermodynamical description, as will be exemplified below.

To find this connection we have to consider the flux of water, $J_w$. The assumption of a steady-state flux implies, via the continuity equation, that $J_w$ is independent of the spatial coordinate. Hence, we find

$$I(\mu_w)\equiv\int_{\xi(\mu_R)}^{\xi(\mu_w)}J_w(\xi)d\xi=J_w(\xi(\mu_w)-\xi(\mu_R)).$$

where the first equality defines the integrated water flux $I(\mu_w)$. Its derivative is, clearly, independent of the lower limit, and we find

$$I'(\mu_w)=J_w\frac{d\xi}{d\mu_w}. \tag{4}$$

We have thus expressed the derivative $\frac{d\xi}{d\mu_w}$ in terms of the function $I'(\mu_w)$, which is known as soon as we have modelled the water flux through the structure. However, we are still missing the constant water flux $J_w$.

To this end we use the condition of constant amount of lipids, and introduce $n_l(\xi)$ as a measure of the amount of lipid at position ξ. The total amount is then given by the integral

$$n_{l\mathrm{Tot}}=\int n_l(\xi)d\xi=\frac{1}{J_w}\int_{\mu_R}^{\mu_D}n_l(\mu_w)I'(\mu_w)d\mu_w$$

where we have used Eq. (4) to go from an integral over ξ to one over $\mu_w$, and again used the assumption of steady state so that $J_w$ can be taken outside the integral. Solving for $J_w$ and using Eq. (4) we can then rewrite Eq. (3) as

$$\frac{1}{P_i}=\frac{n_{l\mathrm{Tot}}}{\int_{\mu_R}^{\mu_D}n_l(\mu_w)I'(\mu_w)d\mu_w}\int_{\mu_R}^{\mu_D}\frac{I'(\mu_w)}{P_i(\mu_w)}d\mu_w. \tag{5}$$

To summarise: Eq. (5) gives a relation between what we measure, the permeability of *i*, and what we control, the water chemical potential (or osmotic pressure). So far this is a general analysis, and we have not assumed anything regarding structure, phases or transport properties. These enter through the local permeability to *i*, $P_i$, the water flux in $I'$, and the local amount of lipids $n_l$. These are all functions of $\mu_w$; in particular they might change discontinuously at the position of phase transition. We now turn to completing the analysis for our specific case by modeling these quantities.

We write the water flux with a generalised Fick's first law [25] as

$$J_w=-\frac{D_w(x)}{RT}c_w(x)\frac{d\mu_w}{dx} \tag{6}$$

Thus the definition of $I'(\mu_w)$, Eq. (4), reads

$$\begin{aligned}I'(\mu_w)&=J_w\frac{d\xi}{d\mu_w}=-\frac{D_w(x)}{RT}c_w(x)\frac{d\xi}{dx}\\&=-\frac{D_w(\mu_w)}{RT}c_w(\mu_w)\frac{1}{l(\mu_w)}\end{aligned} \tag{7}$$

where the last equality uses the definition of the local length $l(\mu_w)$.

Now, if $\mu_w$ is such that it corresponds to the cubic phase, we choose $\xi$ to measure unit cells so that

$$I'(\mu_w) = -\frac{D_w(\mu_w)}{RT}\frac{c_w(\mu_w)}{a(\mu_w)}$$

where $a$ is the size of a unit cell. We further assume ideal solution behaviour $\mu_w = \mu_w^0 + RT \ln c_w/c_w^w$, where $c_w^w$ is the concentration of water in bulk water. The size of the unit cell, $a$ ($\mu_w$) we get from previous thermodynamical modeling of and experiments on the monoolein Ia3d cubic phase [23,31,32] (for details see Supplementary material). For the water diffusion coefficient, $D_w(\mu_w)$, we use NMR measurements of the water self-diffusion coefficient through the monoolein cubic phase [24] (for details see Supplementary material). We find $n_l(\mu_w)$ by assuming a constant area of the membrane $A$ as

$$n_l(\mu_w) = \frac{A}{a^2(\mu_w)} n_{l\mathrm{uc}}(\mu_w) \tag{8}$$

where $n_{l\mathrm{uc}}$ is the amount of lipids of a unit cell, found from the lipid volume fraction [32].

For the lamellar phase, we let $\xi$ measure repeat-spacings, and neglect the gradient in water chemical potential over the water layers. Under this assumption, Eq. (7) reads

$$I'(\mu_w) = -\frac{D_w^l}{RT}\frac{c_w}{2l_m}$$

where $D_w^l$ is the diffusion coefficient of water in the lipid region, and $2l_m$ is the bilayer thickness. If we, again, assume ideal solution behaviour we can rewrite this as [11]

$$I'(\mu_w) = -\frac{K_w D_w^l}{2l_m}\frac{c_w^w e^{(\mu_w-\mu_w^0)/RT}}{RT} = -P_w^{\mathrm{bilayer}}\frac{c_w^w e^{(\mu_w-\mu_w^0)/RT}}{RT}$$

where $K_w$ is the partition coefficient between a lipid phase and an aqueous phase for water, and we have identified the permeability of a lipid bilayer to water, $P_w^{\mathrm{bilayer}}$, in the last step. The latter was estimated as $P_w^{\mathrm{bilayer}} = 3\cdot 10^{-5}$ m/s [33]. The amount of lipids at each bilayer, $n_l$, is, assuming constant density of both water and lipids, given by

$$n_l = 2\frac{A}{A_{l\mathrm{hg}} N_A} \tag{9}$$

irrespective of $\mu_w$, where $A_{l\mathrm{hg}} = 34.7\text{Å}^2$ [27] is the lipid headgroup area.

Fig. 6 shows the effect of the osmotic gradient on the membrane structure under these assumptions.

For the eosin transport, we write the permeability of a unit cell as

$$P_i(\mu_w) = \frac{D_i^{(\mathrm{eff})}}{a(\mu_w)}$$

where $D_i^{(\mathrm{eff})}$ is an effective diffusion coefficient that in general depends on $\mu_w$, but, for simplicity, we have assumed this to be constant. In this approximation the effect of swelling is thus solely manifested in an increase of $a$. For the permeability of the lamellar phase to eosin we note that the inter-bilayer distance is significantly smaller than the bilayer thickness. Furthermore, the partition coefficient of eosin between water and octanol is of the order of $10^{-2}$ [13]. This indicates that the resistance to diffusion is mainly the lipid bilayers, and we approximate $P_i = P_i^{\mathrm{bilayer}}$, where $P_i^{\mathrm{bilayer}}$ is the permeability of a lipid bilayer to eosin.

So far we have not taken into account the porous structure of the support membrane. We have already concluded that there is a negligible influence on the thermodynamic behaviour. Hence, we have assumed the same structure of the cubic phase as in bulk. Also, the position of the phase transition was set to $\Pi = 2.78$ MPa (corresponding to the value found from calorimetric measurements on samples with a monoolein content of 99% [20]) within the range 2.64–3.09 MPa found in bulk measurements above. The swelling of the lamellar phase does not affect the results since we have neglected the resistance to diffusion of both water and eosin over the water layers.

However, as already noted, transport through the porous structure is slower than in bulk due to the tortuosity of the diffusing path. We expect this to influence the permeabilities of the two phases approximately the same, since on a molecular scale the pore orientation is neglible. Thus this will amount to a single pre-factor for the permeability of a unit cell and lipid bilayer, respectively. For the water transport such an effect cancels out, since it is only the *relative* permeability of the two phases that matters, as is readily confirmed from Eq. (5) by including a pre-factor in $I'$. For the eosin transport, though, it does have an effect, but comes out of the integral as a pre-factor to the total permeability (again confirmed by Eq. (5)).

Additionally, we have to account for the fact that the effective area the lipids occupy is smaller in the double-porous membrane than in a pure lipid membrane with the same amount of lipids. Hence the thickness of the volume occupied by the lipids will be thicker, and the permeability lower, even without a tortuous path. Since in the model above $n_l$ for both phases is proportional to the area of the membrane, $A$, this again amounts to a pre-factor to the total permeability (if the $A$ used in Eqs. (8) and (9) is set to the area of the diffusion cell).

Finally, there is a rather subtle effect when one compares the theoretical description with experimental results. The experimental flux of eosin is evaluated by equating the increase in the amount of substance of eosin per unit time with the flux times the area *of the diffusion cell*. However, due to the support membrane the area actually available for transport is less than the area of the diffusion cell. This again amounts to a single pre-factor for the permeability to eosin.

We have shown how all the effects of the porous membrane can be included in a single pre-factor. In principle, this can be found from the structure of the membrane. In practice, however, only an estimate might be possible, though it is clear that with a well-defined structure of the scaffold membrane, less assumptions have to be made in the determination. Regardless of this, the general behaviour is expected to be the same, since this pre-factor only sets the scale.

The result of the model is shown in Fig. 5. Here the total amount of lipids, $n_{l\mathrm{Tot}}$, was estimated from the mass of the lipid per membrane with the help of the ratio of the area of the

diffusion cell to the whole membrane. Furthermore, the effective diffusion coefficient of the cubic phase has been set to $D_i^{(\mathrm{eff})} = 2.1 \cdot 10^{-12}$ m$^2$/s, and the permeability of a lipid bilayer to $P_i^{\mathrm{bilayer}} = 8 \cdot 10^{-8}$ m/s. Both are reasonable values for a polar substance with the size of eosin. With the single pre-factor set to 0.115 – which seems reasonable for the three effects discussed above – we find good agreement with experimental data.

The same values of the two parameters $D_i^{(\mathrm{eff})} = 2.1 \cdot 10^{-12}$ m$^2$/s and $P_i^{\mathrm{bilayer}} = 8 \cdot 10^{-8}$ m/s shows good agreement with the experimental data of Ref. [13] (not shown). Here the osmotic pressures were recalculated with the help of PEG 8000 density measurements [19] and osmotic pressure data [15]. In these experiments the lipid phases were not confined within a porous membrane, and, consequently, no pre-factor 0.115 was used. Furthermore, the position of the phase transition was set to 2.30 MPa, in accordance with the bulk phase behaviour measurements of that batch.

Hence we conclude that the results for the double-porous membrane are consistent with earlier results. However, in contrast to earlier results, the decay of the permeability with the increasing number of bilayers of the lamellar phase is possible to discern in the novel experimental model system. Furthermore, the results can be understood from the presented general model.

## 4. Conclusions

We have shown how a porous polymer membrane can be used as a scaffold for lipid lyotropic phases, thereby creating what we call a *double-porous membrane*. This provides a useful model system for *quantitative* studies on transport through complex barrier membranes. The porous support provides mechanical stability, but may also reduce defects of the lipid lyotropic phases. Furthermore, the interaction between the lipids and the polymer material can result in a surface-induced orientation of anisotropic phases.

In our experiments with monoolein as a model lipid, we found no difference in phase equilibrium inside the porous structure compared to bulk. However, the support membrane induces an orientation of the monoolein liquid crystalline $L_\alpha$ lamellar phase with the bilayer normal parallel to the pore walls. The controlled orientation has a large effect on the quantitative study of transport through the lamellar phase.

Exposure of the double-porous membrane to an externally applied osmotic gradient induces major structural changes within the membrane, and transport through it shows a non-linear response. A major reduction in permeability occurs when there is a phase change between the inverted Ia3d cubic phase and the lamellar phase within the membrane. A general theoretical analysis was given. The special case of a lyotropic phase confined in a porous structure is also specifically treated, and it shows good quantitative agreement with experiment.

The double-porous lipid membrane constitutes a mechanically robust system for studies in aligned systems, which is generally very difficult to achieve. This could have large implications for studies of transport processes in e.g. skin or other biomembrane model systems.

## Acknowledgements

ES acknowledges the Swedish Research Council (Vetenskapsrådet), and FCB the Fundação para a Ciência e para a Tecnologia, Portugal for financial support. We thank Bo Holmström for help with the confocal scanning microscopy measurements, and Peter Linton for help with the SAXS experiments. Finally, we thank Håkan Wennerström for fruitful discussions and helpful critique of the manuscript.

## Appendix A. Supplementary data

Supplementary data associated with this article can be found, in the online version, at doi:10.1016/j.bbamem.2007.10.020.

## References

[1] R.R. Warner, M.C. Myers, D.A. Taylor, Electron probe analysis of human skin: determination of the water concentration profile, J. Invest. Dermatol. 90 (1988) 218–224.
[2] P.M. Elias, Epidermal barrier function: intercellular lamellar lipid structures, origin, composition and metabolism, J. Controlled Release 15 (1991) 199–208.
[3] R.O. Potts, M.L. Francouer, Lipid biophysics of water loss through the skin, Proc. Natl. Acad. Sci. U. S. A. 87 (1990) 3871–3873.
[4] H.E. Boddé, I. van den Brink, H.K. Koerten, F.H.N. de Hann, Visualization of in vitro percutaneous penetration of mercuric chloride; transport through intercellular space versus cellular uptake through desmosomes, J. Control. Release 15 (1991) 227–236.
[5] B.W. Barry, Novel mechanisms and devices to enable successful transdermal drug delivery, Eur. J. Pharm. Sci. 14 (2001) 101–114.
[6] S.H. White, D. Mirejovsky, G.I. King, Structure of lamellar lipid domains and corneocyte envelopes of murine stratum corneum. An X-ray diffraction study, Biochem. 27 (1988) 3725–3732.
[7] M.E. Hatcher, W.Z. Plachy, Dioxygen diffusion in the stratum corneum: an EPR spin-label study, Biochim. Biophys. Acta Biomembr. 1149 (1993) 73–78.
[8] I.H. Blank, J. Moloney III, A.G. Emslie, I. Simon, C. Apt, The diffusion of water across the stratum corneum as a function of its water content, J. Invest. Dermatol. 82 (1984) 188–194.
[9] A. Alonso, N.C. Meirelles, V.E. Yushmanov, M. Tabak, Water increases the fluidity of intercellular membranes of stratum corneum: correlation with water permeability, elastic, and electrical resistance properties, J. Invest. Dermatol. 106 (1996) 1058–1063.
[10] T.K. Mandal, D.T. Downing, Freeze-fracture electron-microscopic and osmotic water permeability studies of epidermal lipid liposomes derived from stratum corneum lipids of porcine epidermis, Acta Derm.-Venereol. 73 (1993) 12–17.
[11] E. Sparr, H. Wennerström, Diffusion through a responding lamellar liquid crystal: a model of molecular transport across stratum corneum, Colloids Surf. B Biointerfaces 19 (2000) 103–116.
[12] E. Sparr, H. Wennerström, Responding phospholipid membranes — interplay between hydration and permeability, Biophys. J. 81 (2001) 1014–1028.
[13] F.O. Costa-Balogh, C. Åberg, J.J.S. Sousa, E. Sparr, Drug transport in responding lipid membranes can be regulated by an external osmotic gradient, Langmuir 21 (2005) 10307–10310.
[14] A. Avdeef, High-throughput measurement of permeability profiles, in: H. van de Waterbeemd, H. Lennernäs, P. Artursson, R. Mannhold (Eds.), Drug Bioavailability: Estimation of Solubility, Permeability, Absorption and Bioavailability, Wiley-VCH, Weinheim, 2003, pp. 46–71.
[15] C.B. Stanley, H.H. Strey, Measuring osmotic pressure of poly(ethylene glycol) solutions by sedimentation equilibrium ultracentrifugation, Macromolecules 36 (2003) 6888–6893.
[16] T. Landh, Phase behavior in the system pine oil monoglycerides-poloxamer 407-water at 20.degree. J. Phys. Chem. 98 (1994) 8453–8467.

[17] S.T. Hyde, S. Andersson, B. Ericsson, K. Larsson, A cubic structure consisting of a lipid bilayer forming an infinite periodic minimum surface of the gyroid type in the glycerolmonooleate-water system, Z. Kristallogr. 168 (1984) 213–219.
[18] J. Briggs, H. Chung, M. Caffrey, The temperature-composition phase diagram and mesophase structure characterization of the monoolein/water system, J. Phys. II 6 (1996) 723–751.
[19] P. González-Tello, F. Camacho, G. Blázquez, Density and viscosity of concentrated aqueous solutions of polyethylene glycol, J. Chem. Eng. Data 39 (1994) 611–614.
[20] E. Sparr, P. Wadsten, V. Kocherbitov, S. Engström, The effect of bacteriorhodopsin, detergent and hydration on the cubic-to-lamellar phase transition in the monoolein–distearoyl phosphatidyl glycerol–water system, Biochim. Biophys. Acta Biomembr. 1665 (2004) 156–166.
[21] T. Landh, Cubic phases and cubosomes in lipid–water systems, Licentiate thesis, Lund University, Lund, Sweden (1991).
[22] H. Qiu, M. Caffrey, The phase diagram of the monoolein/water system: metastability and equilibrium aspects, Biomaterials 21 (2000) 223–224.
[23] H. Chung, M. Caffrey, The curvature elastic-energy function of the lipid–water cubic mesophase, Nature 368 (1994) 224–226.
[24] T. Feiweier, B. Geil, E.-M. Pospiech, F. Fujara, R. Winter, NMR study of translational and rotational dynamics in monoolein–water mesophases: obstruction and hydration effects, Phys. Rev. E 62 (2000) 8182–8194.
[25] D.F. Evans, H. Wennerström, The Colloidal Domain — Where Physics, Chemistry, Biology and Technology Meet, Wiley-VCH, New York, 1999.
[26] J. Engblom, S. Engström, B. Jönsson, Phase coexistence in cholesterol–fatty acid mixtures and the effect of the penetration enhancer azone, J. Control. Release 52 (1998) 271–280.
[27] H. Chung, M. Caffrey, The neutral area surface of the cubic mesophase: location and properties, Biophys. J. 66 (1994) 377–381.
[28] P. Nollert, H. Qiu, M. Caffrey, J.P. Rosenbusch, E.M. Landau, Molecular mechanism for the crystallization of bacteriorhodopsin in lipidic cubic phases, FEBS Lett. 504 (2001) 179–186.
[29] D. Anderson, H. Wennerström, U. Olsson, Isotropic bicontinuous solutions in surfactant–solvent systems: the $L_3$ phase, J. Phys. Chem. 93 (1989) 4243–4253.
[30] J. Crank, The Mathematics of Diffusion, Oxford University Press, Oxford, 1975.
[31] D.M. Anderson, S.M. Gruner, S. Leibler, Geometrical aspects of the frustration in the cubic phases of lyotropic liquid crystals, Proc. Natl. Acad. Sci. U. S. A. 85 (1988) 5364–5368.
[32] D.C. Turner, Z.-G. Wang, S.M. Gruner, D.A. Mannock, R.N. McElhaney, Structural study of the inverted cubic phases of di-dodecyl alkyl-β-D-glucopyranosyl-*rac*-glycerol, J. Phys. II 2 (1992) 2039–2063.
[33] Y. Graziani, A. Livne, Water permeability of bilayer lipid membranes: sterol-lipid interaction, J. Membr. Biol. 7 (1972) 275–284.